ON THE SWITCHED RELUCTANCE LINEAR MOTOR POSITIONING SYSTEM CONTROL

Ioan-Adrian VIOREL - SZABÓ Loránd - KOVÁCS Zoltán

Technical University of Cluj
Department of Electrical Engineering
P.O. Box 358, 3400 Cluj-Napoca, ROMANIA
Fax:+40-64-192035
E-mail: Ioan.Adrian.Viorel@mae.utcluj.ro
Lorand.Szabo@mae.utcluj.ro

ABSTRACT

Variable speed linear drives including also positioning tasks play an important role in modern industries. Such drives have to be robust, rugged, maintenance free, intelligent and must assure high accuracy with good efficiency. The adequately designed and controlled switched reluctance linear motor (SRLM) can offer a good solution for such a drive. This paper proposes and analyses, based on computer simulation, such a drive. The SRLM mathematical model is briefly presented. A simplified motor model allows the optimum command position determination. An intelligent controller is proposed based on the control strategy that follows from the theoretical approach. The results obtained via computer simulation stand by to sustain the pertinence of the aimed solution.

1. INTRODUCTION

Translations are the most common motions in several industrial branches. Usually the linear motion is generated by belt or spindle drives using rotational motors. Elasticity and gear backlash limit the dynamics as well as the accuracy of such drives. These mechanical arrangements allow for low speed only. Utilization of high performance linear motors can eliminate these disadvantages because they generate linear motion without any extra mechanical components. There are no specific couplings and the produced traction force is directly acting on the load. The switched reluctance linear motor (SRLM) is one of the linear motors that can be used in such drives. The adequately designed SRLM commanded via an intelligent controller can realize high stiffness and good dynamics.

The switched reluctance motors, with true electronic commutation, synchronized with rotor position on its rotative variant, have been described in the early seventies. Since then many improvements have been done and now the switched reluctance motor is a vigorous competitor for variable speed drive systems. The SRLM comes up with the same features as the rotative one. It has low manufacturing costs, rugged and robust construction, simple and reliable power switching circuits. This motor has also some notable weakness, like variation of the tangential force over a wide range, function of the command currents and position. The normal forces are significant, too, and impose an adequately built suspension system.

The SRLM is a multi-phase, single side excited, electronically commutated variable reluctance motor. It is double salient with an unequal number of platen and mover poles. In Fig. 1 the four phases short mover SRLM is presented. The mover iron core is built by using laminated sheets. The four coils are wounded around the mover salient poles, each being supplied from a PWM type power electronic converter. The platen is a toothed block constructed of magnetically soft material. It can be built up of laminated sheets, too, in order to reduce eddy current losses and parasitic forces. The tangential force is achieved by supplying adequately the mover's command coils. This force is produced by the tendency of a platen pole to align with the mover's pole that has the maximum amperturns. The mover tooth pitch is 1.75 times greater than the platen tooth pitch.

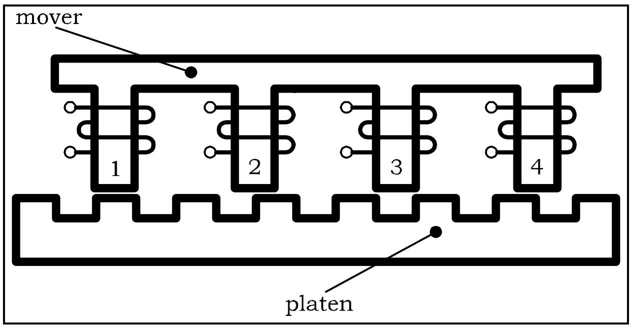

Figure 1

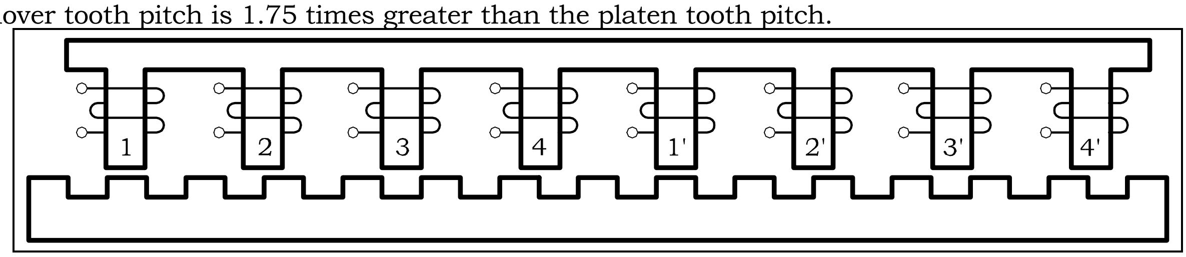

Figure 2

In Fig. 2 a long mover, four phases SRLM is presented. Each phase of the motor is compounded by connecting in series the coils wound around the symmetrical mover poles. The phase *A*, for instance, is obtained by connecting in series the coils *1* and *1'*. There are no other differences, as construction is concerned, between the two motors. Their operating principle is the same, too.

To achieve the high performances expected from a variable speed positioning drive system, the SRLM requires an instantaneous force control. Hence, the command current will be adequately provided by the power electronic converter in order to obtain the prescribed traction force. This force must be as smooth as possible, which means low force ripples. The command current waveform is specific for a given motor and depends on the drive imposed operating conditions. The SRLM being a self-commutated motor, the command current commuting moment depends on the mover's position related to the platen.

The SRLM mathematical model lays on the base of its control strategy. Therefore the motor model is developed and the theoretical results are utilized to obtain the control system basics. Finally, in the paper the proposed drive system is simulated on computer. The obtained results stand by to prove the effectiveness of the drive system, which can be a valuable alternative to a similar system using hybrid linear stepper motors.

2. MATHEMATICAL MODEL

Mathematical modeling provides a convenient way of describing electrical machine's behavior. Costly experiments regarding the machine response to different operating conditions can be cheaply overpassed by simulating the machine based on the developed mathematical model.

The SRLM exhibits strong nonlinearities due to the nonsinusoidal variation of the phase inductance function of the mover position and due to the current-dependent iron core saturation that depends on the mover position, too. Therefore the air-gap flux must be computed at each mover position and for the corresponding command current value. It can be done via a circuit-field-mechanical model, which covers accurately the effects of complex toothed configuration and the magnetic saturation of the iron core parts [1]. The block diagram of this model is shown in

Fig. 3. The three submodels and their connections are outlined. In this circuit-field-mechanical model, first developed for the linear hybrid stepper motor [1], the field submodel is based on the equivalent magnetic circuit of the motor.

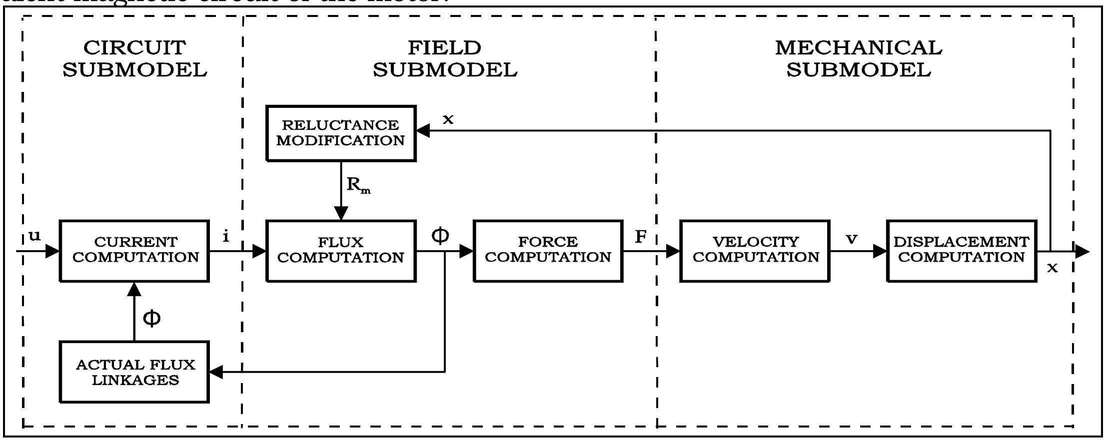

Figure 3

Obviously the field problem may be solved via a numerical method, using finite elements, or finite differences modes. Most computer packages are developed based on the finite elements method (FEM). The FEM approach takes into account the nonlinear magnetic properties of the utilized ferromagnetic materials and the detailed geometry of both motor parts. The solution, consisting of the magnetic potential values in the considered domain, allows the appropriate evaluation of the flux linkages, tangential and normal forces, losses, energy, co-energy and inductances. The FEM is very accurate, but requires long computation time and therefore is not well suited for dynamic simulations.

By using the equivalent magnetic circuit method the flux linkage throughout the motor is computed for certain command currents. Within this method the entire motor structure is divided into small portions having the same magnetic properties. The iron core nonlinear magnetic characteristics are fully taken into account. The variation of the air-gap magnetic reluctance under the motor poles function of the mover position is considered, too.

There are some different possibilities to calculate the air-gap permeance when both iron cores of the motor have tooth and slots in cylindrical or linear machines. The method proposed here comes up as an extension of the method developed for the hybrid linear stepper motor [2]. If the coordinate system axes are taken into the axis of symmetry of the mover, then the equivalent variable permeances considering slots and teeth only on the mover, respectively on the platen are:

$$P_{m_1}(x) = \begin{cases} \dfrac{1+\lambda_1}{2k_{c_1}g}\left\{1+\cos\left[Z_2(x+\alpha)\right]\right\}, & x+\alpha \in \left[\dfrac{\pi}{Z_1}-\dfrac{\pi}{Z_2};\dfrac{\pi}{Z_1}+\dfrac{\pi}{Z_2}\right] \\ 0, \quad x+\alpha \in \left[0;\dfrac{\pi}{Z_1}-\dfrac{\pi}{Z_2}\right)\cup\left(\dfrac{\pi}{Z_1}+\dfrac{\pi}{Z_2};\dfrac{2\pi}{Z_1}\right] \end{cases} \tag{1}$$

$$P_{m_2}(x) = \frac{1}{k_{c_2}g}\left(1-\lambda_2\cos x\right) \tag{2}$$

where λ_1, λ_2 are the coefficients of the equivalent variable air-gap permeance [3], k_{c_1}, k_{c_2} are the Carter's factors, Z_1, Z_2 are the number of the teeth (poles) on the mover, respectively platen. g is the air-gap length, x the geometric displacement and α the variable displacement between the two axes considered on the mover and platen.

The air-gap equivalent variable permeance results:

$$P_m(x) = P_{m_1}(x) P_{m_2}(x) g \tag{3}$$

and the average specific permeance under one pole is given by:

$$P_{m_a} = \frac{Z_1}{2\pi} \int_{\frac{\pi}{Z_1} - \frac{\pi}{Z_2}}^{\frac{\pi}{Z_1} + \frac{\pi}{Z_2}} P_m(x) dx \tag{4}$$

which leads to

$$P_{ma_j} = \frac{1}{g'} P_0 \left[1 - b \cos\left(Z_2 \alpha_j + \pi / Z_1\right)\right] \qquad j = 1 \div 4 \tag{5}$$

where:

$$P_0 = \frac{Z_1}{Z_2} \frac{1 + \lambda_1}{2} \qquad b = \frac{\lambda_2}{2} \qquad g' = k_{c_1} k_{c_2} g \tag{6}$$

The tangential force developed under pole number *j* is:

$$f_{t_j} = -\left(\frac{\partial W_{m_j}}{\partial x}\right)_{\Phi_j = ct.} \qquad j = 1 \div 4 \tag{7}$$

The magnetic co-energy is given by the following relation:

$$W_{m_j} = \frac{\Phi_j^2}{2\mu_0 S} \frac{g'}{P_0 \left[1 - b \cos\left(Z_2 \alpha_j + \pi / Z_1\right)\right]} \qquad j = 1 \div 4 \tag{8}$$

and the force expression is:

$$f_{t_j} = \frac{\Phi_j^2}{2\mu_0 S} \frac{g' \sin\left(Z_2 \alpha_j + \pi / Z_1\right)}{P_0 \left[1 - b \cos\left(Z_2 \alpha_j + \pi / Z_1\right)\right]^2} \frac{Z_2}{Z_1} \frac{2\pi}{\tau_1} \qquad j = 1 \div 4 \tag{9}$$

where S is the mover pole area, τ_1 is the mover pole pitch and μ_0 is the free space permeability ($\mu_0 = 4\pi 10^{-7} \mathrm{H / m}$).

The normal force developed under the mover's pole number *j* is:

$$f_{n_j} = -\left(\frac{\partial W_{m_j}}{\partial g}\right)_{\Phi_j = ct.} = -\frac{\Phi_j^2}{2\mu_0 S} \qquad j = 1 \div 4 \tag{10}$$

The mechanical submodel is characterized by the equation:

$$m \frac{d^2 x}{dt^2} = f_t - \left(f_n + G\right) \mu_f \tag{11}$$

where μ_f is the friction coefficient, G the mover's weight, m the mover mass and f_t, f_n the total tangential, respectively normal force.

The mechanical submodel considered here is a simplified one based on the following assumptions:

i) The motor is a homogenous solid. The resulting tangential and normal forces are applied on its center.

ii) The resulting forces are obtained by summing algebraic the pole forces.

This simplified mechanical model does not take into account the existing torque produced by the normal forces applied in each pole axe.

In the field submodel the nonlinear permeances of the motor iron core portions must be computed by means of the corresponding field-dependent single valued permeability μ. The dependence of the permeability μ is obtained by calculus at each iteration from the given magnetizing characteristic of the iron core material.

In order to obtain analytical results, which prove to be helpful in building up the control strategy, two simplifying assumptions must be considered:

i) The motor iron core is not affected by saturation.

ii) The air-gap reluctances are larger than all other reluctances.

The equivalent magnetic circuit of the short mover motor having command coil current only through pole number two coil is given in Fig. 4. The mover position is corresponding to that shown in Fig. 1. The air-gap flux can be computed from the equivalent magnetic circuit:

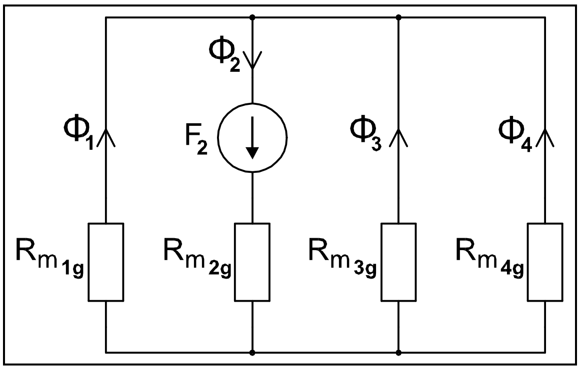

Figure 4

$$\Phi_1 = \frac{F_2}{R_{m_{1g}} + R_{m_{2g}}} \qquad \Phi_3 = \frac{F_2}{R_{m_{2g}} + R_{m_{3g}}} \qquad \Phi_4 = \frac{F_2}{R_{m_{2g}} + R_{m_{4g}}} \tag{12}$$

$$\Phi_2 = \Phi_1 + \Phi_3 + \Phi_4 = F_2\left(\frac{1}{R_{m_{1g}} + R_{m_{2g}}} + \frac{1}{R_{m_{2g}} + R_{m_{3g}}} + \frac{1}{R_{m_{2g}} + R_{m_{4g}}}\right) \tag{13}$$

The tangential and normal forces can be computed with relations (9), and respectively (10), substituting the corresponding flux, for instance:

$$f_{t_1} = \frac{1}{2} F_2^2 \frac{R'_{m_{1g}}}{\left(R_{m_{1g}} + R_{m_{2g}}\right)^2} \tag{14}$$

$$f_{n_1} = -\frac{\Phi_1^2}{2\mu_0 S} \tag{15}$$

The air-gap reluctances are given by the relation:

$$R_{m_{jg}} = \frac{g'}{2\mu_0 S} \frac{1}{P_0\left[1 - b\cos\left(Z_2\alpha_j + \pi/Z_1\right)\right]} \qquad j = 1 \div 4 \tag{16}$$

and the reluctance derivative is:

$$R'_{m_{1g}} = \frac{\partial R_{m_{1g}}}{\partial x} \qquad (17)$$

It is clear that at each time moment the force equilibrium equation (14) is solved with the values of the forces computed at the previously moment of time.

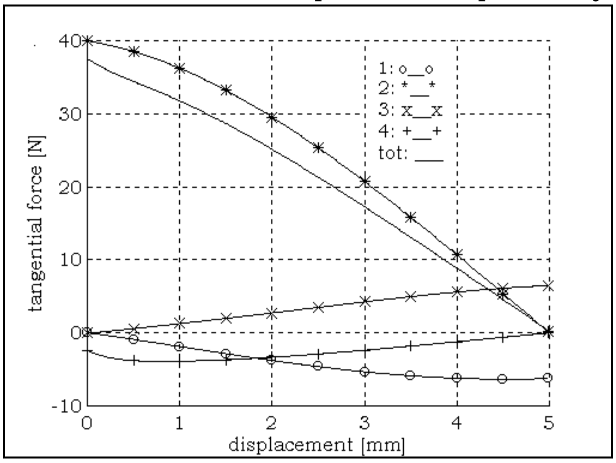

Figure 5

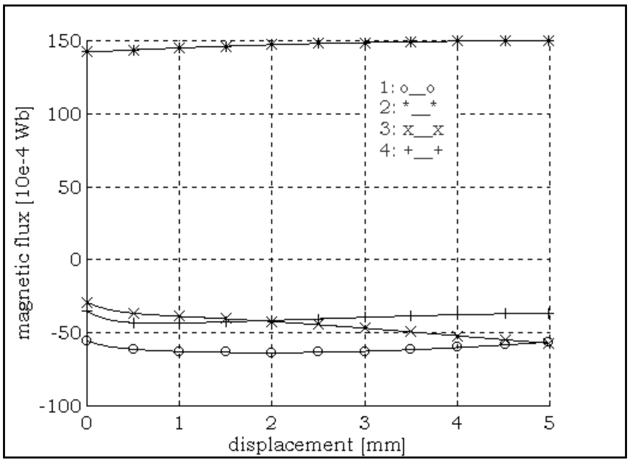

Figure 6

The tangential forces and the corresponding air-gap flux linkages of the sample motor (see Appendix 1), computed for constant exciting current are shown in Fig. 5., and respectively Fig. 6.

The forces f_1 and f_3 are starting from zero, the first being a breaking one. The f_2 force is at its maximum value at the beginning and decreases as does the force f_4, which has the opposite sign and a smaller value.

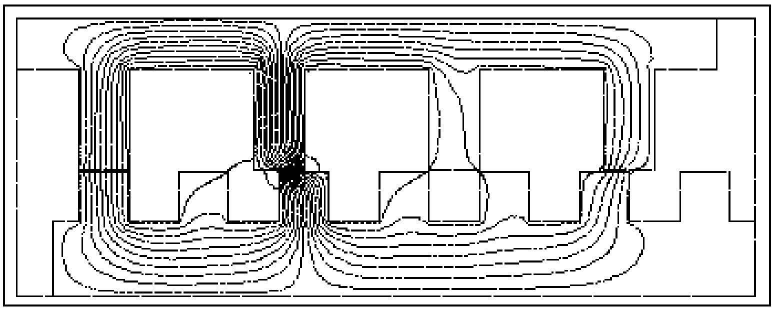

Figure 7

In Fig. 7 the plotted magnetic field is given, plotted for the same case and initial position. It wae obtained by using MAGNET 5.2 package. The figure demonstrates that the results obtained via the FEM analysis perfectly agree with the theoretical anticipations.

The air-gap induction is shown in Fig. 8. As it can be seen the air-gap induction is varying far from the sinusoidal waveform adopted in the permeance computation process.

It means that the tangential forces computed through the simplified model just presented are smaller and the flux under the unexcited poles are larger. The differences, evidenced in another paper [4], are not so important, therefore the briefly presented mathematical model can be of real help in simulating dynamic processes of the SRLM.

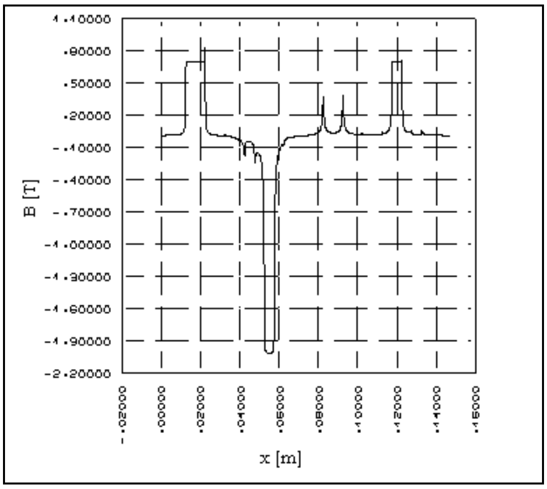

Figure 8

3. CONTROL STRATEGY

The dynamic performance of the motor can be improved by an adequate control strategy, implemented in the system controller. The control system has to offer, in certain limits, the possibility to maintain a prescribed speed and to assure a corresponding positioning task. In order to realize the requirements imposed on the SRLM dynamics the optimum moment of the motor phases commutation must be computed and the mover position related to the platen must be determined as accurate as possible.

The optimum moment of the motor phases commutation corresponds to the maximum value of the average total tangential force developed during a control sequence. The total tangential force generated is given by the following relation:

$$f_t = \sum_{j=1}^{4} f_{tj} \tag{18}$$

where the expression of the tangential force is given in (14) for the first pole of the SRLM, when only coil number two is supplied. The SRLM position is corresponding to that shown in Fig. 1, and the equivalent magnetic circuit is that given in Fig. 4. It results:

$$\begin{aligned} f_t = \frac{1}{2} F_2^2 \frac{1}{\left(R_{m2g}+R_{m3g}\right)^2} \Bigg\{ & \left(\frac{R_{m2g}+R_{m3g}}{R_{m1g}+R_{m2g}}\right)^2 \left(R'_{m1g}+R'_{m2g}\right) + \\ & + \left(R'_{m2g}+R'_{m3g}\right) + \left(\frac{R_{m2g}+R_{m3g}}{R_{m2g}+R_{m4g}}\right)^2 \left(R'_{m2g}+R'_{m4g}\right) + \\ & + 2R'_{m2g} \left[\frac{R_{m2g}+R_{m3g}}{R_{m1g}+R_{m2g}} + \frac{R_{m2g}+R_{m3g}}{R_{m2g}+R_{m4g}} + \frac{\left(R_{m2g}+R_{m3g}\right)^2}{\left(R_{m1g}+R_{m2g}\right)\left(R_{m2g}+R_{m4g}\right)} \right] \Bigg\} \end{aligned} \tag{19}$$

The average tangential force is:

$$f_{t_a} = \frac{1}{\tau_s} \int_{x_0-\tau_s/2}^{x_0+\tau_s/2} f_t \, dx \tag{20}$$

where τ_s is the SRLM's step length. Usually it is equal to half of the mover's pole width,

$$\tau_s = w_s/2 \tag{21}$$

The optimal commutation position is obtained from the equation:

$$\frac{df_{t_a}}{dx_0} = 0 \tag{22}$$

The system of equations (19), (20) and (22) can be solved analytically by a numerical method.

If the excitation MMF is commutated from one phase to another at the optimum command position, the tangential force will be smooth, with low ripple, having the maximum average value. The commutation at the optimum moment offers the possibility to control the SRLM’s speed by regulating only the excitation currents.

The induced EMF in the unenergized coils can be of real help in determining the mover's position related to the platen. The already presented case will be considered, when only the coil from the pole number two is supplied. The induced EMF in the other three phases are:

$$e_1 = -N\frac{d\Phi_1}{dt} = NF_2 \frac{R'_{m_{1g}} + R'_{m_{2g}}}{\left(R_{m_{1g}} + R_{m_{2g}}\right)^2}\frac{d\alpha}{dt} \tag{23}$$

$$e_3 = -N\frac{d\Phi_3}{dt} = NF_2 \frac{R'_{m_{2g}} + R'_{m_{3g}}}{\left(R_{m_{2g}} + R_{m_{3g}}\right)^2}\frac{d\alpha}{dt} \tag{24}$$

$$e_4 = -N\frac{d\Phi_4}{dt} = NF_2 \frac{R'_{m_{2g}} + R'_{m_{4g}}}{\left(R_{m_{2g}} + R_{m_{4g}}\right)^2}\frac{d\alpha}{dt} \tag{25}$$

All the phases have the same number of turns in series, N, and the derivates are function of time. This means:

$$\frac{dR_{m_{1g}}}{dt} = \frac{\partial R_{m_{1g}}}{\partial \alpha}\frac{d\alpha}{dt} = R'_{m_{1g}}\frac{d\alpha}{dt} \tag{26}$$

where

$$\alpha = \frac{2\pi}{Z_1\tau_1}x \qquad \frac{d\alpha}{dt} = \frac{2\pi}{Z_1\tau_1}\frac{dx}{dt} \tag{27}$$

There are several combinations of induced EMFs in unenergized coils which do not depend on the mover's speed and excitation MMF. For instance:

$$\frac{e_3}{e_4} = \frac{R'_{m_{2g}} + R'_{m_{3g}}}{R'_{m_{2g}} + R'_{m_{4g}}}\left(\frac{R_{m_{2g}} + R_{m_{4g}}}{R_{m_{2g}} + R_{m_{3g}}}\right)^2 \tag{28}$$

The equation (28) allows for computing the mover position related to the platen. It means that by monitoring the induced EMF in the unenergized coils the mover position can be detected without any special sensors.

The induced EMF e_3 and e_4 were considered, because through these two phases are not flowing currents when the supply is commutated from one phase to another. It must be mentioned here the fact that the expressions for e_3 and e_4, (24) and (25), are not depending on the existence of current in phase number one.

The control strategy now is clear. The position of the mover is detected by monitoring the induced

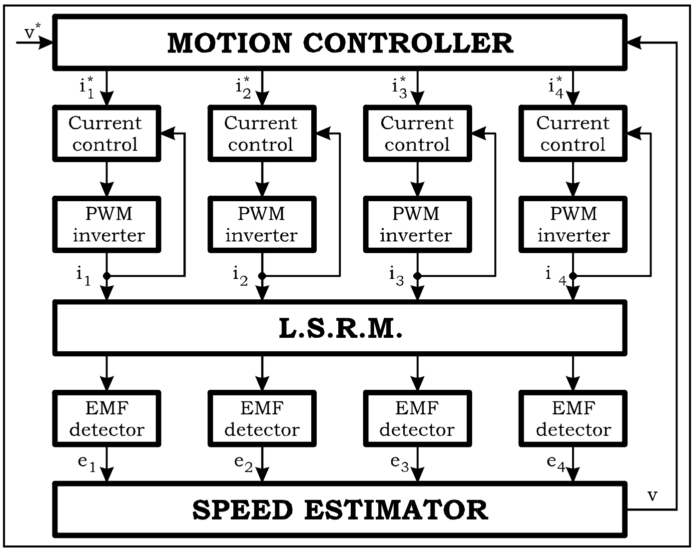

Figure 9

EMF through the unenergized coils. The commutation will take place at the optimum moment, function of the mover's position. The SRLM's speed control is obtained by controlling the excitation current via a PWM electronic converter.

A possible hard structure of the system that realizes this control strategy is presented in Fig. 9. The moment when the commutation is performed can be different of the optimum one. This moment is computed for a specific SRLM, taking into account its data and it must be introduced in the controller. It is possible to change this commutation moment upon a prescribed rule, in order to control the resulting tangential force.

If positioning is the main task of the system, then quite a different strategy must be adopted. First it is necessary to provide the SRLM with a position sensor. It must have a good accuracy, because the positioning precision relies on it.

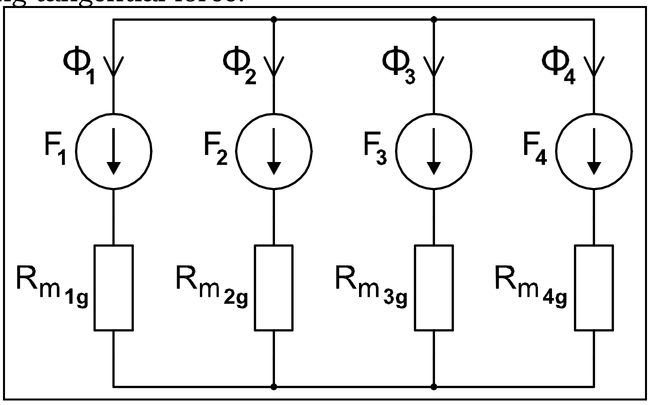

Figure 10

Beside this a different way of exciting the SRLM's phases must be adopted. At least two phases must be supplied simultaneously, but a higher accuracy will be achieved by supplying all four phases in the same time with different currents. In this case the equivalent magnetic circuit attached to the motor is shown in Fig. 10. By such a supplying strategy the tangential force can be controlled adequately and brought to zero at any position of the mover. Each tangential force is depending at least of two excitation currents. For example, the force developed under the mover's pole number one is:

$$f_{t_1} = \frac{1}{2}\left(F_1 + F_2\right)^2 \frac{R'_{m_{1g}}}{\left(R_{m_{1g}} + R_{m_{2g}}\right)^2} \tag{29}$$

Unfortunately such a strategy implies a complicated controller. The induced EMF sensing cannot be utilized in this case, because all of the phases are supplied. Therefore a special positioning sensor must be provided, as it was stated before. The total tangential force is larger, as it can be seen from the results of the simulation presented in the following section.

4. RESULTS AND CONCLUSIONS

A computer program was developed on the base of the circuit-field-mechanical model. It allows the calculation of all the SRLM's important characteristics, such as the tangential and normal forces, mover's displacement and speed, phase currents, flux linkages in the air-gap and in the irqqon core and so on. Some particular cases were considered, too.

The excitation currents were taken ideals: in the turn on phases the currents come to their maximum value intantantaneously and they are constants during the whole conducting period. When the phases are turned off the currents are coming to zero also instantaneously. Results for such a case are given in Figs. 5 and 6, when only phase number two is supplied. Two other similar cases were considered. The tangential force variations versus the mover's displacement are given in Figs. 11 and 12. In the first case only a single phase is supplied at a moment. The commutation was done at the optimum moment. In the other case two coils were supplied simultaneously.

Finally, a simple positioning task was simulated. Only one phase was supplied at a moment. The current decay in the phase turned off was taken into account, too. The control system is that proposed in this paper. The mover position is detected by monitoring the induced EMF in the unenergized phases A trapezoidal speed profile was adopted. Some of the

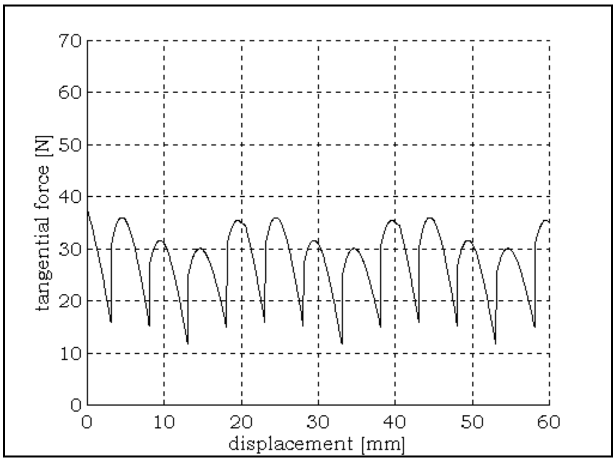

Figure 11

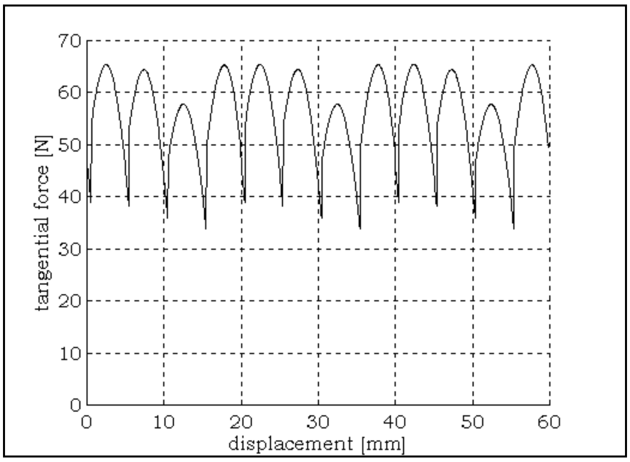

Figure 12

obtained results are presented in the given plots: the resulting tangential force (Fig. 13), the mover's velocity and displacement (Figs. 14 and 15).

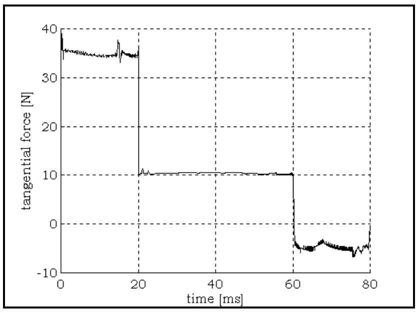

Figure 13

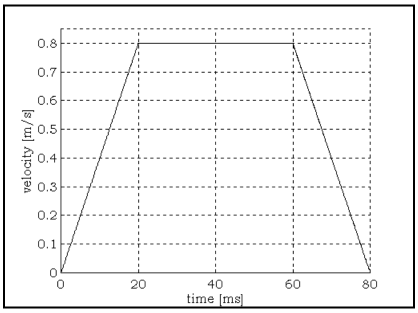

Figure 14

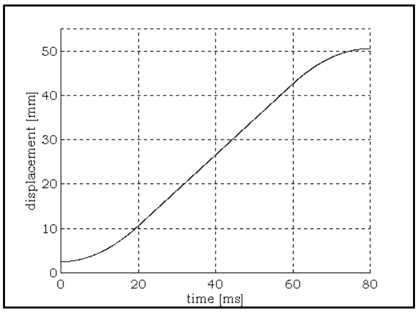

Figure 15

As it can be seen from the presented results, the SRLM is a good competitor in variable speed linear drive systems. It compensates the not so high performances by robustness and very low cost.

APPENDIX

The characteristics of the sample motor

ITEM	VALUE	ITEM	VALUE
platen tooth width	10mm	platen slot width	10mm
mover pole width	10mm	mover slot width	25mm
pole length	20mm	motor thickness	85mm
number of turns of coils	750	command current	2.5A

REFERENCES

1. VIOREL I.A. et al.: **Sawyer Type Linear Motor Modelling**, Proceedings of the International Conference on Electrical Machines 1992, pp. 697-701.
2. VIOREL I.A. - SZABÓ L.: **Hybrid Linear Stepper Motors**, Mediamira Publishing House, Cluj-Napoca, Romania, 1998
3. Jufer M. et al.: **On the Switched Reluctance Motor Air-Gap Permeance**, Proceedings of the ELECTROMOTION International Symposium, 1995, pp. 141-146
4. VIOREL I.A. et al.: **On the Switched Reluctance Linear Motor Mathematical Model**, Paper to be published in the Oradea University Annals, 1998